Unbreakable $\mathcal{PT}$-symmetry and its consequence in a $\mathcal{PT}$-symmetric dimer

J Ramya Parkavi[iD] and V K Chandrasekar[1] [iD]

Centre for Nonlinear Science & Engineering, School of Electrical & Electronics Engineering, SASTRA Deemed University, Thanjavur-613 401, Tamilnadu, India

E-mail: ramyaparkji@gmail.com and chandrasekar@eee.sastra.edu

CrossMark

Abstract

This article presents a finite dimensional unbreakable $\mathcal{PT}$-symmetric waveguide system with linear and nonlinear coupling. In traditional $\mathcal{PT}$-symmetric systems, a balance (or a symmetric state) among the waveguides with loss and gain can be achieved only when the coupling among the waveguides is sufficiently strong. But the coupled waveguide system that we report here obtains the balance (or symmetry preservation) as soon as the couplings are established and this symmetric nature is undisturbed even for arbitrarily large values of loss–gain strength. We here show that the $\mathcal{PT}$-symmetry in the system is unbreakable in the presence of linear and nonlinear coupling. Interestingly, in the absence of linear coupling, the system shows contrast behavior where $\mathcal{PT}$-symmetry is spontaneously broken for all parametric values. As the considered system is integrable, we illustrate the symmetry unbroken and broken nature of the system using their integrals of motion. Importantly, we illustrate the possibility to have high power oscillations by weakening the couplings among the waveguides.

Keywords: unbreakble PT-symmetry, integrability, power amplifiers

(Some figures may appear in colour only in the online journal)

1. Introduction

Hybridizing many features of conservative and dissipative systems, the class of $\mathcal{PT}$-symmetric systems stand unique and open up new prospects for better control over physical processes [1–4]. For instance, in optical systems, the non-reciprocal nature of $\mathcal{PT}$-symmetric systems enable active light control which gives hope for the development of all-optical devices on a micro-scale optical chip [5–7]. The robustness of $\mathcal{PT}$-symmetric systems in cavity mode selection evidences its advantage in single mode microlasers [8, 9] and consequently

---

[1]Author to whom any correspondence should be addressed.

in the development of next-generation optoelectronic devices for optical communications. Similarly, the applications of $\mathcal{PT}$-symmetric systems are not limited to optics, interesting phenomena have been observed in other fields including acoustics [10, 11], plasmonics [12, 13], quantum optics of atomic gases [14, 15], Bose–Einstein condensates in optical lattices [16] and electronic circuits [17].

A typical phenomenon observed in these $\mathcal{PT}$-systems is that spontaneous breaking of $\mathcal{PT}$-symmetry which leads to two different phases, namely, unbroken and broken $\mathcal{PT}$-phases. In the unbroken $\mathcal{PT}$-phase, these systems often behave similar to that of conservative systems and support stationary solutions. Non-conservative features can be seen in the broken $\mathcal{PT}$-phase which appears for higher gain–loss strength. From the application point of view, both phases are interesting [1, 18–20] and various experimental investigations have been carried to capture the symmetry breaking phenomena and to study the characteristics of the system in the two phases [21–24]. Eventhough the spontaneous symmetry breaking is observed in many of the $\mathcal{PT}$-symmetric systems, there are few special cases in which the symmetry is unbreakable and the system remains in unbroken $\mathcal{PT}$-phase for arbitrarily large values of gain–loss strength [25–27].

Such unbreakable $\mathcal{PT}$-symmetric systems are reported mainly in the case of infinite dimensional systems where the unbroken $\mathcal{PT}$-phase features a special class of self-trapped solutions. Because the self-organized solutions supported by traditional dissipative systems are of attractor type [28, 29] but the ones supported by $\mathcal{PT}$-symmetric systems form a continuous family of solutions as observed in the conservative systems [30, 31]. In [32], the authors have introduced the 2D network of $\mathcal{PT}$-symmetric dimers with cubic nonlinearity. Due to its unbreakable $\mathcal{PT}$-symmetric nature, the system supports stable symmetric fundamental solitons at lowest power and anti-symmetric fundamental soliton and vortices at high powers were observed. As symmetry breaking limits the parametric regions of stable $\mathcal{PT}$-symmetric solitons, the explorations of unbreakable $\mathcal{PT}$-symmetric systems have got interest [25–27]. Considering finite dimensional systems, unbroken $\mathcal{PT}$-phase features power oscillations [18, 33, 34] which can be used in applications like two-way switches [35]. As far as we know, the finite dimensional example of unbreakable $\mathcal{PT}$-symmetry is given only by I V Barashenkov and M Gianfreda in [36]. They have reported the unbreakable $\mathcal{PT}$ symmetric nature in a particular case of Hamiltonian $\mathcal{PT}$ symmetric dimer (where gain and loss strength alone serves as a free parameter) and shown the existence of stable high amplitude oscillations at higher gain–loss strength. More explorations of finite dimensional systems with intact $\mathcal{PT}$-symmetry is required.

In the above context, we report a finite dimensional coupled waveguide system with intact $\mathcal{PT}$-symmetry and study the consequences of unbreakable $\mathcal{PT}$-nature in the system. The considered $\mathcal{PT}$-system with loss and gain has linear and nonlinear couplings and the presence of either of the couplings is sufficient for the system to be $\mathcal{PT}$-symmetric. In the absence of linear coupling, the symmetry of the system is strictly broken whilst it is unbreakable for all parametric values in the presence of linear coupling. The symmetry is intact even for finite (but non-zero) values of linear and non-linear couplings and also for arbitrarily larger values of loss–gain strength. This seems to be interesting because in the absence of linear and nonlinear coupling, the two waveguides, respectively, with gain and loss shows dissipative dynamics where one of the waveguide shows abrupt growth and the other shows decay in power [37]. Thus, the propagation of stationary and also symmetric modes is expected only for sufficiently strong coupling (either linear or nonlinear coupling or both) among the waveguides. This article shows that as a consequence of unbreakable $\mathcal{PT}$-nature, the considered waveguide system supports stable symmetric modes even for weaker linear and nonlinear couplings and also the observed symmetric modes in such parametric regime are of high power.

Thus, due to the intact $\mathcal{PT}$-symmetric nature, we obtain high power oscillations through weakening the coupling strengths and there is no need to have high loss and gain. We hope that exploration of this type of systems can lower the switching power if the observed power oscillations were utilized for switching applications (as low input power is sufficient to obtain the high power oscillation) [35]. On the other hand, they may also be used for optical amplification [38, 39].

In this article, we explain the above mentioned characteristics of the system with the use of their integrable nature. In section 2, we first present the considered model. The complete asymmetric nature of the $\mathcal{PT}$-symmetric system in the absence of linear coupling is elucidated in section 3. As the latter case is exactly solvable, the existence of symmetry broken solutions are elucidated via exact solutions and this case also presents an interesting dynamical aspect where the existence of isochronous oscillations are shown. Now introducing the linear coupling section 4, the sudden disappearance of asymmetric modes and the stabilization of symmetric mode is shown through the linear stability analysis of nonlinear modes. To deepen our understanding of the latter case, we present the integrable nature of the system in section 5. As the linear stability analysis is a local analysis, it provides only qualitative information about the system, the integrals of motion presented in the latter section enables us to figure out (i) the initial conditions that can lead to power oscillations and the ones lead to blow-up responses and (ii) the maxima and minima of the power oscillations. With these as tools, we presented the dynamics of the waveguide coupler for weaker and stronger coupling strengths in section 6 and discussed the consequence of the unbreakable $\mathcal{PT}$-symmetric nature. Finally, the obtained results have been summarized in the section 7.

2. Model

Consider a coupled waveguide problem in which the propagation of light in the waveguides is described by the following coupled mode equations

$$i\frac{d\phi_1}{dz} = \omega\phi_1 - i\gamma\phi_1 + i\alpha(|\phi_1|^2 + |\phi_2|^2)\phi_1 + k\phi_2,$$

$$i\frac{d\phi_2}{dz} = \omega\phi_2 + i\gamma\phi_2 - i\alpha(|\phi_2|^2 + |\phi_1|^2)\phi_2 + k\phi_1. \tag{1}$$

In the above, ϕ_1 and ϕ_2 are the complex amplitudes of electromagnetic field that describe the propagation of light in the two waveguides with respect to the propagation direction z. The parameter ω represents the propagation constant, γ is the linear loss–gain strength, k is the evanescent field coupling and α represents the strength of nonlinearity. Here, we can also observe a nonlinearity involving total power in the third term of equation (1). In this nonlinear term, the first part of the term represents a nonlinear loss–gain nature and the second part of the term represents a nonlinear coupling among the waveguides which may be achieved through stimulated Raman scattering as discussed in [40–42].

It is interesting to note that the above system is integrable and is also exactly solvable in the case of $k = 0$. Below, we elucidate the integrable nature and show the interesting dynamics observed in the $k = 0$ and $k \neq 0$ cases.

3. Asymmetric modes in the absence of linear coupling

In this section, we study the field dynamics of the coupler (1) in the absence of linear coupling and present the existence of an interesting asymmetric mode. In general, one may not achieve

waveguide coupler without linear coupling but very recently, the researchers have also shown the possibility to have complete nonlinear coupling (without linear coupling) among resonators [43]. Thus we hope that this system with purely nonlinear coupling may also be achieved with proper experimental set-up and this section presents some interesting dynamical aspects of a $\mathcal{PT}$-symmetric system (note the system is $\mathcal{PT}$-symmetric even in the absence of linear coupling).

To understand the field propagation in this case, we utilize the exactly solvable nature of the system. The details of solving the considered case and the integrals of motion associated with the case has been given in appendix A. From the latter, the general solution of the system can be written as

$$\phi_1 = \sqrt{P_1}e^{-i\omega z + i\theta}, \quad \text{and} \quad \phi_2 = \frac{Ce^{-i\omega z - i\theta}}{\sqrt{P_1}}, \tag{2}$$

where,

$$P_1 = \frac{\gamma}{2\alpha} + \frac{\sqrt{\gamma^2 - 4\alpha^2|C|^2}}{2\alpha}\left(\frac{e^{-2\sqrt{\gamma^2 - 4\alpha^2|C|^2}z} + C_3}{e^{-2\sqrt{\gamma^2 - 4\alpha^2|C|^2}z} - C_3}\right). \tag{3}$$

In the above, $C = C_1 + iC_2$, C_3 and θ are integral constants. Note that $P_1 \in \mathfrak{R}$ (so $\gamma^2 - 4\alpha^2|C|^2 \geqslant 0$) and so the solution represents the system dynamics only when $|C|^2 \leqslant \frac{\gamma^2}{4\alpha^2}$. For the initial conditions corresponding to $|C|^2 \geqslant \frac{\gamma^2}{4\alpha^2}$, P_1 can be written as

$$P_1 = \frac{\gamma}{2\alpha} + \frac{\sqrt{4\alpha^2|C|^2 - \gamma^2}}{2\alpha}\tan\left(\frac{\sqrt{4\alpha^2|C|^2 - \gamma^2}}{\alpha}(z + \tilde{C}_3)\right). \tag{4}$$

From the above solutions (3) and (4), we observe that the latter solution corresponding to $|C|^2 \geqslant \frac{\gamma^2}{4\alpha^2}$ represents blow-up response (due to the presence of tan function) and so the power in the waveguides tend to infinity as $z \to \infty$. But the former one given in (3) represents a stable solution and the power in the two waveguides at the asymptotic limit (P_1^A and P_2^A) can be written as

$$P_1^A = |\phi_1^A|^2 = \frac{\gamma}{2\alpha} - \frac{\sqrt{\gamma^2 - 4\alpha^2|C|^2}}{2\alpha},$$

$$P_2^A = |\phi_2^A|^2 = \frac{\gamma}{2\alpha} + \frac{\sqrt{\gamma^2 - 4\alpha^2|C|^2}}{2\alpha},$$

$$\phi_{1,2}^A = \sqrt{P_{1,2}^A}e^{-i\omega z + i\theta}. \tag{5}$$

The above expression represent that in the asymptotic limit ϕ_1 and ϕ_2 exhibit a periodic oscillations with frequency ω (same as the frequency of the linear oscillation). Note that the frequency of these oscillations does not depend on the initial conditions or the amplitude of oscillation which denotes the isochronous nature of the oscillations. We have presented the dynamics corresponding to solution (2) in figures 1(a) and 1(b) where one can observe periodic oscillations after a short transient.

A closer look at equation (5) indicates that P_1^A and P_2^A vary with respect to initial conditions but the total asymptotic power does not depend on initial condition, that is,
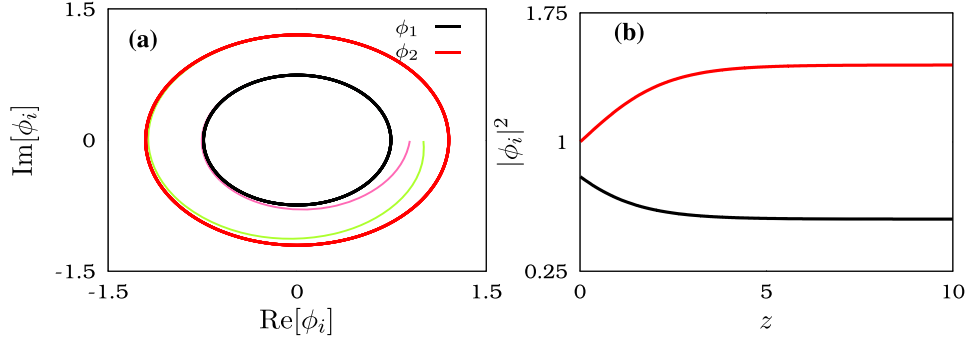
$$P_1^A + P_2^A = \frac{\gamma}{\alpha}. \tag{6}$$

Figure 1. For $\gamma = 1.0$, $\alpha = 0.5$ and $k = 0$, the above figures (a) and (b) respectively represent the dynamics of the complex amplitudes ϕ_1 and ϕ_2 and the intensity at the two waveguides $|\phi_1|^2$ and $|\phi_2|^2$. In figure (a), the thin pink and green lines represents the transient dynamics before the system settles into the orbit.

The above expressions (5) and (6) indicate that P_1^A and P_2^A respectively can take the values only in the range $\frac{\gamma}{2\alpha} \geqslant P_1^A \geqslant \frac{\gamma}{\alpha}$ and $0 \geqslant P_2^A \geqslant \frac{\gamma}{2\alpha}$ (and so $P_1^A \geqslant P_2^A$). Thus, the amplitudes of oscillations P_1^A and P_2^A are restricted even though they are continuous. In addition, $P_1^A \neq P_2^A$ represents the asymmetric nature of the modes. But, for the initial conditions corresponding to $|C|^2 = \frac{\gamma^2}{4\alpha^2}$, the modes become symmetric where $P_1^A = P_2^A = \frac{\gamma}{2\alpha}$.

4. No more asymmetry in the presence of linear coupling

Now, we focus on the dynamics of the system for k non-zero case. As similar to the previous one, this case is also found to be integrable but not exactly solvable. It is non-trivial to express their exact solution explicitly and so we first study the dynamical characteristics by examining the stationary modes corresponding to the system and by studying their stability. We present the details of their integrable nature and the understandings derived out from it in the next section.

Considering the stationary modes of the system, firstly the linear modes corresponding to the systems are stable for $k \geqslant \gamma$. To find the nonlinear modes corresponding to the system, we consider

$$\phi_1 = R_1 e^{-i\tilde{\omega}z + i\theta_1}, \quad \phi_2 = R_2 e^{-i\tilde{\omega}z + i\theta_2}, \tag{7}$$

and substituting the above in equation (1) leads to

$$\dot{R}_1 + i\dot{\theta}_1 R_1 = -\gamma R_1 + \alpha(R_1^2 + R_2^2)R_1 - ikR_2 e^{-i(\theta_1 - \theta_2)},$$
$$\dot{R}_2 + i\dot{\theta}_2 R_2 = \gamma R_2 - \alpha(R_1^2 + R_2^2)R_2 - ikR_1 e^{i(\theta_1 - \theta_2)}. \tag{8}$$

Decomposing the real and imaginary parts of the above equation, we obtain

$$\dot{R}_1 = -\gamma R_1 + \alpha(R_1^2 + R_2^2)R_1 - kR_2 \sin(\theta_1 - \theta_2),$$
$$\dot{R}_2 = \gamma R_2 - \alpha(R_1^2 + R_2^2)R_2 + kR_1 \sin(\theta_1 - \theta_2),$$
$$\dot{\theta}_1 R_1 = -kR_2 \cos(\theta_1 - \theta_2), \quad \text{and} \quad \dot{\theta}_2 R_2 = -kR_1 \cos(\theta_1 - \theta_2). \tag{9}$$

From the latter set of equations, we find $\left(\dot{\theta}_1 - \dot{\theta}_2\right) = k\frac{(R_1^2 - R_2^2)}{R_1 R_2}\cos(\theta_1 - \theta_2)$. Defining the phase difference $\delta = \theta_1 - \theta_2$, we can write the equations of amplitude and phase as

$$\dot{R}_1 = -\gamma R_1 + \alpha(R_1^2 + R_2^2)R_1 - kR_2 \sin \delta,$$

$$\dot{R}_2 = \gamma R_2 - \alpha(R_1^2 + R_2^2)R_2 + kR_1 \sin \delta,$$

$$\dot{\delta} = k\frac{(R_1^2 - R_2^2)}{R_1 R_2} \cos \delta. \tag{10}$$

Before we look at the modes corresponding to the k nonzero case, we check the modes corresponding to $k = 0$ case and is of the form

$$R_1^{*2} + R_2^{*2} = \frac{\gamma}{\alpha}, \quad \delta^* = \text{constant}. \tag{11}$$

It is very obvious that it is same as the one given in equation (6).

Now with the introduction of k, the nonlinear modes corresponding to the system are of the form,

$$R_1^* = R_2^* = R^*, \quad \sin \delta^* = \frac{2\alpha R^{*2} - \gamma}{k}, \tag{12}$$

where, R^* can take any positive real values but the fact, $|\sin\delta| \leqslant 1$, restricts the value of R^*. Due to this reason, R^* can take the values between

$$\sqrt{\frac{\gamma - k}{2\alpha}} \leqslant R^* \leqslant \sqrt{\frac{\gamma + k}{2\alpha}} \quad \text{while } k < \gamma,$$

$$0 \leqslant R^* \leqslant \sqrt{\frac{\gamma + k}{2\alpha}} \quad \text{while } k \geqslant \gamma. \tag{13}$$

We can also note that, $R_1^* = R_2^*$ denotes that they are symmetric and stabilization of such modes give rise to the symmetry unbroken phase. Note that the existence of asymmetric mode ceases while k is non-zero. Thus to find the stable or unstable nature of this mode, we did linear stability analysis and the results indicate that the eigenvalues corresponding to these symmetric modes are

$$\lambda = 0, \pm 2\sqrt{\gamma^2 - k^2 - 6\gamma\alpha R_2^2 + 8\alpha^2 R_2^4}. \tag{14}$$

The eigenvalues indicate that whenever the term inside the squareroot is negative, that is, when $A_- < R^* < A_+$ where $A_\pm = \sqrt{\frac{3\gamma \pm \sqrt{\gamma^2 + 8k^2}}{8\alpha}}$, the symmetric mode can become neutrally stable. Combining the above criteria with the allowed values of R^* given in equation (13), we find that the symmetric mode is neutrally stable for all non-zero values of parameters (including k) with R^* lying in the range $\sqrt{\frac{\gamma - k}{2\alpha}} \leqslant R^* \leqslant A_+$ while $k < \gamma$ and $0 \leqslant R^* \leqslant \sqrt{\frac{\gamma + k}{2\alpha}}$ while $k \geqslant \gamma$. This denotes $\mathcal{PT}$-symmetry of the system is unbreakable. This has also been illustrated in figure 2.

This stable nature of the symmetric mode for both lower and higher values of coupling strengths k and α is notable as the possibility to obtain balance of power between the loss and gain sites at very weaker coupling is surprising. Thus it is important to observe the dynamics of the systems with respect to different coupling strengths in particular for the lower coupling regime. As the linear stability analysis is a local analysis, its results picture the nature of the
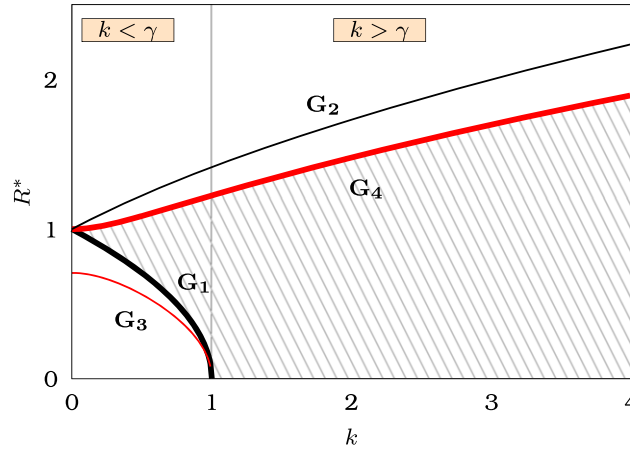
Figure 2. The shaded region in the figure presents the values of R^* for which the symmetric mode exists with pure imaginary eigenvalues. Here, the curves G_1 and G_2 respectively represent the curves $R^* = \sqrt{\frac{\gamma - k}{2\alpha}}$ and $R^* = \sqrt{\frac{\gamma + k}{2\alpha}}$. The curves G_3 and G_4 represent $R^* = A_-$ and $R^* = A_+$.

system for initial conditions near to the stationary mode given in equation (12). To have a wide view and to have complete picture with respect to initial conditions, we here utilize the integrable nature of the system and illustrate the consequence of unbreakable $\mathcal{PT}-$ symmetry.

5. Integrable nature

The integrable nature of the considered system can be understood clearly when we look upon the dynamics in terms of the Stokes variables [44, 45], namely,

$$p = |\phi_1|^2 + |\phi_2|^2, \quad s_0 = |\phi_1|^2 - |\phi_2|^2, \quad s_1 = \phi_1\phi_2^* + \phi_1^*\phi_2,$$
$$s_2 = i(\phi_1\phi_2^* - \phi_1^*\phi_2) \quad \text{with } p^2 = s_0^2 + s_1^2 + s_2^2. \tag{15}$$

In terms of these new real variables, the dynamical equation of the system can be written as

$$\dot{p} = -2(\gamma - \alpha p)s_0, \quad \dot{s_0} = -2(\gamma - \alpha p)p + 2ks_2,$$
$$\dot{s_1} = 0, \qquad\qquad \dot{s_2} = -2ks_0. \tag{16}$$

The above equation has two integrals of motion and an obvious integral of motion is

$$s_1 = I_1 = \text{constant}. \tag{17}$$

The other one can be written as (see appendix B for details)

$$(\gamma - \alpha p)e^{\frac{\alpha}{k}s_2} = I_2 = \text{constant}. \tag{18}$$

The presence of two integrals of motion I_1 and I_2 associated with the system given in equation (16) ensures the integrable nature of the system. From the above integrals given in

equations (17) and (18) and from the relation that exists between the variables (equation (15)), one can obtain the below form of equation,

$$\dot{p}^2 = 4(\gamma - \alpha p)^2 \left[p^2 - I_1^2 - \left(\frac{k}{\alpha} \ln \left(\frac{\gamma - \alpha p}{I_2} \right) \right)^2 \right] \tag{19}$$

which is similar to the classical Hamiltonian corresponding to a particle in a potential well $V(p)$. In more clear words, we can view the above expression in the form,

$$\frac{\dot{p}^2}{2} + V(p) = 0, \tag{20}$$

where,

$$V(p) = 2(\gamma - \alpha p)^2 \left[I_1^2 + \left(\frac{k}{\alpha} \ln \left(\frac{\gamma - \alpha p}{I_2} \right) \right)^2 - p^2 \right]. \tag{21}$$

Eventhough it is non-trivial to write the explicit solution of equation (19), the above potential picture enable us to understand the dynamics of the system from the turning points p_t (corresponding to $V(p_t) = 0$) and fixed points p^* (corresponding to $V'(p^*) = 0$) of the potential mentioned in equation (21). For the simple form of initial conditions such as $\phi_1(0) = 0$ or $\phi_2(0) = 0$ corresponding to $I_1 = 0$, the turning points of this logarithmic potential can be written simply as,

$$\text{TP}_1 : p_t = \frac{\gamma}{\alpha}, \tag{22}$$

$$\text{TP}_2 : p_t = \frac{\gamma + kW\left(\frac{-I_2 e^{-\frac{\gamma}{k}}}{k} \right)}{\alpha}, \tag{23}$$

$$\text{TP}_3 : p_t = \frac{\gamma - kW\left(\frac{I_2 e^{\frac{\gamma}{k}}}{k} \right)}{\alpha}. \tag{24}$$

$W(X)$ in equations (23) and (24) represents product log function or Lambert-W function and this W function yields real quantity only when $x > \frac{-1}{e}$. For other initial conditions corresponding to $I_1 \neq 0$, the expression of TP$_1$ remains same but the explicit expressions of TP$_2$ and TP$_3$ are non-trivial to present here. The minima corresponding to the potential can also be obtained from $V'(p*) = 0$. One obvious potential minima is $p^* = \frac{\gamma}{\alpha}$ which is nothing but $\frac{\gamma}{\alpha}$ and the other one corresponds to $(\gamma - \alpha p) \left(\frac{kI_2}{(\gamma - \alpha p)} \ln \left(\frac{\gamma - \alpha p}{I_2} + p \right) \right) + \alpha \left(I_1^2 + \left(\frac{k}{\alpha} \ln \left(\frac{\gamma - \alpha p}{I_2} \right) \right)^2 - p^2 \right) = 0.$

6. Dynamics in the system of unbreakable $\mathcal{PT}$-symmetry

6.1. Dynamics at lower k: existence of symmetric oscillations

With these, we now improve our understanding on the dynamics of the systems using the numerical schemes and by using the above potential picture. To start with, we consider the case of focus, that is, the case of smaller k and fix γ and α respectively as 1.0 and 0.5. In view of the illustration purpose, we consider the simple form of initial condition $\phi_1(0) \neq 0$ and $\phi_2(0) = 0$ (and so $I_1 = 0$ and $I_2 = \gamma - \alpha p(0)$). The numerical solution corresponding to
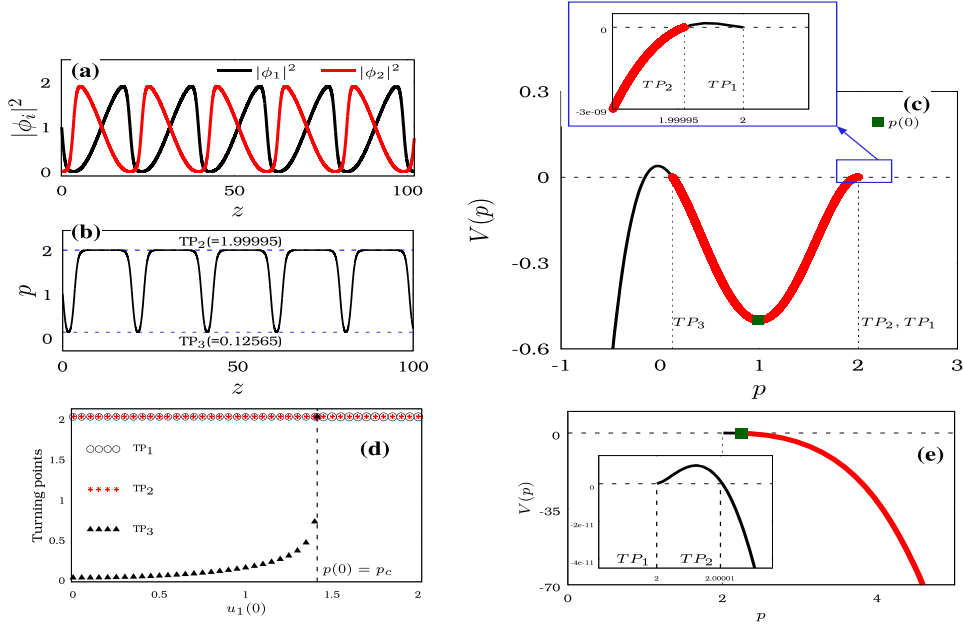
Figure 3. Figures (a)–(e) demonstrates the dynamics of the system for $\gamma = 1.0$, $\alpha = 0.5$ and $k = 0.1$. Figures (a) and (b) are respectively the plots of $|\phi_i|^2$, $i = 1, 2$ and total power (p) with respect to z for the initial condition $\phi_1(0) = 1.0$ and $\phi_2(0) = 0.0$. The corresponding potential $V(p)$ curve given in equation (21) is plotted in figure (c) where the thick red curve denotes the dynamics of the system between the turning points TP$_2$ and TP$_3$. The sub-plot in figure (c) is used to clearly distinguish TP$_1$ and TP$_2$. Figure (d) pictures out the values of turning points for different initial conditions and here the initial condition ($\phi_j(0) = u_j(0) + i v_j(0)$, $j = 1, 2$) is varied in such a way that $u_1(0)$ is alone varied and we have kept $u_2(0) = v_{1,2}(0) = 0$ for simplicity. The potential curve has been plotted in figure (e) in the region where TP$_3$ ceases to exist, that is, for $u_1(0) = 2.5$.

such a case ($k = 0.1$) is given in figure 3(a) where one can surprisingly find the existence of symmetric power oscillations for this lower value of k. As mentioned above, the dynamics can also be understood well from the potential picture [42, 45, 46]. To illustrate the above, we have plotted figures 3(b) and (c) respectively elucidating the dynamics of total power and the potential picture illustrating the latter dynamics. Considering figure 3(c), the thin black curve represents the structure of the logarithmic potential given in equation (21) for the considered parametric values and initial conditions. One can observe that the potential $V(P)$ exists between $p = 0$ and 2 and it becomes complex for $p > 2$. The dynamics of the system can also be inferred from the structure of the potential and the turning and fixed points of the system, where the total power of the system exhibits oscillations about the potential minima or fixed point located at $p^* = 1.0$. Note that eventhough $p(0)(= 1.0)$ matches with p^* (in this particular case), $\dot{p}(0)$ does not match with $\dot{p}^*$ and the turning points TP$_2$ and TP$_3$ acts as extrema of their dynamics (the inset in figure 3(c) clearly shows that the dynamics is between TP$_2$ and TP$_3$ and not TP$_1$ and TP$_3$). This can also be confirmed from the numerical result given in figure 3(b). In this figure, we note that the values of TP$_2$ and TP$_3$ act as maxima and minima values of the power oscillations.

Being confirmed the existence of symmetric oscillation for lower k value, we now turn our attention toward the dynamics for different initial conditions. We vary the value of $u_1(0)$
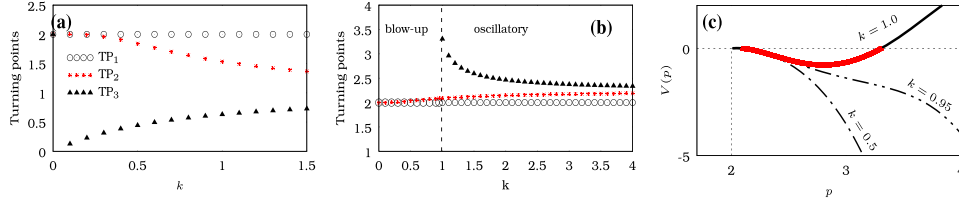
Figure 4. Figures (a) and (b) figures out the turning points of $V(p)$ for different values of k with $\gamma = 1.0$ and $\alpha = 0.5$. In figures (a) and (b), we respectively considered the initial situations (a) $\phi_1(0) = 1.0$ and $\phi_2(0) = 0.0$ and (b) $\phi_1(0) = 1.5$ and $\phi_2(0) = 0.0$. Here, the turning points TP_1–TP_3 have been notated with the same legends used in figure 3. In figure (c), we have considered $\phi_1(0) = 1.5$ and $\phi_2(0) = 0.0$ and shown how k changes the structure of the potential $V(p)$. Note that the potential corresponding to $k = 0.5$ and 0.95 indicates blow-up dynamics and the one corresponding to $k = 1.0$ indicate oscillatory type dynamics.

(where $u_1(0) = \mathrm{Re}[\phi_1(0)]$ and we let $\mathrm{Im}[\phi_1(0)] = 0$) and plotted the values of the turning points in figure 3(d). The turning points TP_1 and TP_2 are located in close proximity with each other so that they are not clearly separated in figure 3(d). Considering TP_3, it shows significant changes with respect to the variation of $u_1(0)$ or equivalently $p(0)$ and it reaches the value of 2 at $u_1^2(0) = p(0) = \frac{\gamma}{\alpha} = 2$. Increasing $u_1(0)$ further, we find that at a critical value, namely, $u_1(0) = u_c$ or $p(0) = p_c$, TP_3 ceases to exist as it becomes complex and equation (24) indicates that this critical value is

$$p_c = \frac{\gamma}{\alpha} + \frac{k}{\alpha}\mathrm{e}^{-\frac{(\gamma+k)}{k}}. \tag{25}$$

The annihilation of the turning point TP_3 has greater impact over the dynamics (as the previous case (figures 3(a)–(c)) shows that the symmetric oscillations were observed between TP_2 and TP_3) where blow-up responses have been observed for those initial conditions. The potential structure corresponding to such initial condition ($u_1(0) = 1.5 > u_c$) is figured out in 3(e), where one can observe that the potential is complex upto $p < 2$ and it is real for $p \geqslant 2$. TP_1 and TP_2 are located closed with each other (near $p = 2$), the inset of figure 3(e) clearly shows the location of the two turning points. It is obvious from figure 3(e) that a fictitious particle placed at the point $p(0)$ (marked by dark-green square) will slide down along the potential leading to blow-up response.

Thus we can summarize here that eventhough the symmetric oscillations exists for lower values of k, we can also observe blow-up responses for certain initial conditions. For the situations $I_1 = 0$, we can find that symmetric oscillations were observed for $p \leqslant p_c$ and blow-up responses for $p > p_c$. With these ideas, we now move onto the dynamics of the system for higher values of k.

6.2. Dynamics for higher k: suppression of blow-up regimes

Now we increase the value of k and look upon the dynamics of the system. To elucidate the impact of strengthening k, we here plot the turning points of the potential with respect to k for two different initial conditions (i) $\phi_1(0) = 1.0$ and $\phi_2(0) = 0.0$ (the situation in which we observed oscillatory dynamics in the case of figure 3) (ii) $\phi_1(0) = 1.5$ and $\phi_2(0) = 0.0$ (the situation in which we observed blow-up response in the case of figure 3) in figures 4(a) and (b). From figure 4(a), we observe that by the increase of k, TP_2 starts diverging from the value of TP_1 and the values of TP_3 also show changes. Thus, strengthening of k alters the maxima and
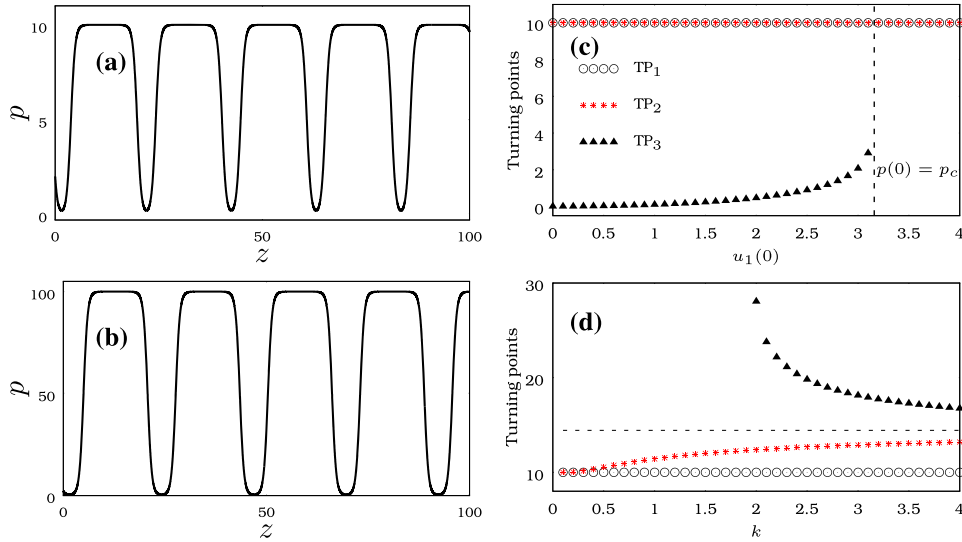
Figure 5. Figures (a) and (b): high power oscillation observed in the coupled waveguide system respectively for $\alpha = 0.1$ and $\alpha = 0.01$. Figure (c) elucidates the variation of turning points with respect to initial condition $u_1(0)$, where we considered $\phi_1(0) = u_1(0) + 0i$, $\phi_2(0) = 0$ and $\alpha = 0.1$. In figure (d), for the same value of α, we have drawn the variation of turning points with respect to k and elucidated the control of blow-up response for $\phi_1(0) = 3.8$ and $\phi_2(0) = 0.0$. In all the figures, we have considered $\gamma = 1.0$ and $k = 0.1$.

minima of the power oscillations. As maxima value (position of TP_2) of the power oscillations decreases with the increase of k, comparatively higher power light transport can be observed for lower k.

Considering figure 4(b), we observe that the increase of k changes the blow-up dynamics to power oscillations through the entry of TP_3. This is because that increasing the value of k, the critical value p_c also increases. Thus the suppression of blow-up regimes and emergence of oscillatory dynamics happens because of the strengthening of k. It is also important to note here these oscillations observed for initial conditions $p(0) > \frac{\gamma}{\alpha}$, TP_3 is found to be the maxima of power oscillation and TP_2 acts as minima of the power oscillation. In the figure 4(c), we have clearly figured out how the potential changes with respect to the value of k and how it support oscillations for higher k.

6.3. Lowering both linear and nonlinear coupling strengths

Eventhough the previous section elucidates the possibility of the gain and loss sites to balance themselves to produce sustained power oscillations for smaller values of k, still the nonlinear coupling α is not weak. In such a case, the stronger nonlinear coupling may also help to balance the gain and loss present in the coupled waveguide sites. Thus the obvious question is here that what happens to the beam propagation pattern if both linear and nonlinear couplings were considered to be weak. The results of the linear stability analysis indicates that the symmetry is unbreakable (and symmetric power oscillations) for all values of $\alpha \neq 0$ and $k \neq 0$. Thus in figure 5(a), we look upon the dynamics of total intensity for $\gamma = 1.0$, $k = 0.1$ and $\alpha = 0.1$ and importantly we here observe a high power oscillations even for less intense input power $\phi_1(0) = 1.0$ and $\phi_2(0) = 0.0$. By recalling the fact that for lower values of k,

the value of TP$_2$ is approximately close to $\frac{\gamma}{\alpha}$ (or TP$_2$ is closer to TP$_1$). The value of TP$_2$ (maxima of the power oscillation) increases significantly with respect to the reduction of α. For instance, the high intense light transport for $\gamma = 1.0$ and $\alpha = 0.01$ (where, $\frac{\gamma}{\alpha} = 100$) is also demonstrated in figure 5(b). Thus it denotes that in the presence of weaker couplings, the tendency of the non-conservative nature of the waveguide sites in growing the intensity of the sites in combination with the symmetry unbreakable nature of the system allows to have sustained high power oscillations. This makes obvious that the unbreakable $\mathcal{PT}$-symmetric nature may open-up new possibilities for light amplification.

By varying the input powers, we have also presented the turning points of the system for $\gamma = 1.0$, $\alpha = 0.1$ and $k = 0.1$ in figure 5(c). In this figure, as k is considered to be small, TP$_2$ and TP$_1$ are closer to each other (at $\frac{\gamma}{\alpha}$). The other important thing that can be noted here is that the value of TP$_2$ does not change significantly with respect to $u_1(0)$, thus for any input powers $p(0) < p_c$, here we can obtain power oscillations with maxima to be at 10.

Considering an initial condition corresponding to blow-up response in figure 5(d) (that is, $u_1(0) = 3.8$), we have captured the values of the turning points for different values of k. As seen earlier, the increase in k leads to the emergence of TP$_3$ and gives rise to power oscillations.

7. Summary

In this article, we have presented a $\mathcal{PT}$-symmetric coupled waveguide system with linear (k) and nonlinear (α) coupling. In the absence of the linear coupling, the system does asymmetric transport of light. By introducing linear coupling, we expected that the asymmetric state retain its stability upto a critical value of k and stabilizes symmetric modes afterward. But, we have observed that the stabilization of the symmetric mode occur as quickly as the linear coupling is introduced and the asymmetric states also cease to exist with its presence. The symmetric state is found to be stable for all values of k, γ, $\alpha \neq 0$, indicating the unbreakable $\mathcal{PT}$-symmetric nature. Besides the balance between the linear and nonlinear loss–gain, the balance between the nonlinear loss–gain and the nonlinear coupling present in the system equation (1) plays a key role in such $\mathcal{PT}$ preservation. Because, this type of intact $\mathcal{PT}$-symmetric nature cannot be seen in the cases where the balance of the latter nonlinear terms are absent. We have studied the consequence of this unbreakable $\mathcal{PT}$-symmetric nature. Our results show that the non-conservative nature of the waveguide sites and the unbreakable nature of the $\mathcal{PT}$-symmetry aids in the generation of high power oscillation for lower coupling strengths. We hope that such generation of high powers with unbreakable $\mathcal{PT}$-symmetric systems may find fruitful application in optical amplifiers and low power applications.

The considered system is integrable and this integrable nature helped to understand the dynamics of the system in the initial condition space more clearly. We have shown that eventhough the symmetric power oscillations were observed for all values of parameters, the blow-up responses also do exist for certain initial conditions. For a class of initial conditions corresponding to $I_1 = 0$ (which is possible for either $\phi_1(0) = 0$ or $\phi_2(0) = 0$), we have figured out the basin of attraction of symmetric mode ($p(0) < p_c$) and the initial conditions that lead to blow-up response ($p(0) > p_c$).

Acknowledgment

Appendix A. Solvability of $k = 0$ case

To solve equation (1), we simplify it by considering

$$\phi_1 = \psi_1 e^{-i\omega z}, \quad \phi_2 = \psi_2 e^{-i\omega z}. \tag{A.1}$$

Now the system in equation (1) (for $k = 0$) can be reduced to

$$i\dot{\psi}_1 = -i\gamma\psi_1 + i\alpha(|\psi_1|^2 + |\psi_2|^2)\psi_1$$
$$i\dot{\psi}_2 = i\gamma\psi_2 - i\alpha(|\psi_2|^2 + |\psi_1|^2)\psi_2 \tag{A.2}$$

From the above, it is obvious that $\frac{d(\psi_1\psi_2)}{dz} = 0$ so that

$$\psi_1\psi_2 = C; \quad C = C_1 + iC_2, \quad C_1, C_2 \in \Re \tag{A.3}$$

is integral of motion of the system (A.2). The complex nature of this integral constant enables one to reduce the order of the differential equation by two (with $\psi_2 = \frac{C}{\psi_1}$) and so one can now simply consider

$$i\dot{\psi}_1 = -i\gamma\psi_1 + i\alpha\left(|\psi_1|^2 + \frac{|C|^2}{|\psi_1|^2}\right)\psi_1. \tag{A.4}$$

Now to solve the above equation, we consider

$$\psi_1 = \sqrt{P_1}e^{i\theta_1}, \quad \psi_2 = \sqrt{P_2}e^{i\theta_2} \tag{A.5}$$

and decompose the equation (A.4) into equations of amplitude and phase as given below

$$\dot{P}_1 = -2\gamma P_1 + 2\alpha(P_1^2 + |C|^2), \quad \dot{\theta}_1 = 0. \tag{A.6}$$

The above equation (A.6) denotes the phase factor θ_1 is a constant of motion ($\theta_1 = \theta = $ constant) and the equation of corresponding to P_1 can also be solved easily and its solution is presented in the main text (equations (3) and (4)).

Appendix B. Integral motion at $k \neq 0$

To derive equation (18), consider the first and fourth equations of equation (16) and so the equation becomes

$$\frac{\dot{s}_2}{k} = \frac{\dot{p}}{\gamma - \alpha p} \tag{B.1}$$

Integrating on both sides of the equation, we get

$$\frac{s_2}{k} = \frac{-1}{\alpha}\left[\ln(\gamma - \alpha p) + \ln(I_2)\right] \tag{B.2}$$

Then by using logarithmic rules,

$$\frac{\alpha s_2}{k} = \ln\left(\frac{I_2}{\gamma - \alpha p}\right) \tag{B.3}$$

Rearranging the terms one can obtain,

$$(\gamma - \alpha p)e^{\frac{\alpha s_2}{k}} = I_2 = \text{constant} \tag{B.4}$$

where I_2 is the integrals of motion.

ORCID iDs

J Ramya Parkavi ⓘ https://orcid.org/0000-0002-5012-8753
V K Chandrasekar ⓘ https://orcid.org/0000-0002-2220-9310

References

[1] Konotop V V, Yang J and Zezyulin D A 2016 Nonlinear waves in PT-symmetric systems *Rev. Mod. Phys.* **88** 035002
[2] Suchkov S V, Sukhorukov A A, Huang J, Dmitriev S V, Lee C and Kivshar Y S 2016 Nonlinear swithcing and solitons in PT-symmetric photonic systems *Laser Photonics Rev.* **10** 177
[3] Zhao H and Feng L 2018 Parity-time symmetric photonics *Natl. Sci. Rev.* **5** 183–99
[4] Sukhorukov A A, Xu Z and Kivshar Y S 2010 Nonlinear suppression of time reversals in $\mathcal{PT}$-symmetric optical couplers *Phys. Rev.* A **82** 043818
[5] Liu Y, Hao T, Li W, Capmany J, Zhu N and Li M 2018 Observation of parity-time symmetry in microwave photonics *Light: Sci. Appl.* **7** 38
[6] Peng B, Özdemir S K, Lei F, Monifi F, Gianfreda M, Long G L, Fan S, Nori F, Bender C M and Yang L 2014 Nonreciprocal light transmission in parity-time-symmetric whispering-gallery microcavities *Nat. Phys.* **10** 394
[7] Wen J, Jiang X, Jiang L and Xiao M 2018 Parity-time symmetry in optical microcavity systems *J. Phys. B: At. Mol. Opt. Phys.* **51** 222001
[8] Ren J, Liu Y G N, Parto M, Hayengo W E, Hokmabadi M P, Christodoulides D N and Khajavikhan M 2018 Unidirectional light emission in PT-symmetric microring lasers *Opt. Express* **26** 27153–60
[9] Feng L, Wong Z J, Ma R, Wang Y and Zhang X 2014 Single-mode laser by parity-time symmetry breaking *Science* **346** 972–5
[10] Zhu X, Ramezani H, Shi C, Zhu J and Zhang X 2014 PT -symmetric acoustics *Phys. Rev.* X **4** 031042
[11] Yang Y, Jia H, Bi Y, Zhao H and Yang J 2019 Experimental demonstration of an acoustic asymmetric diffraction grating based on passive parity-time-symmetric medium *Phys. Rev. Appl.* **12** 034040
[12] Benisty H *et al* 2011 Implementation of PT symmetric devices using plasmonics: principle and applications *Opt. Express* **19** 18004–19
[13] Lupu A, Benisty H and Degiron A 2013 Switching using PT symmetry in plasmonic systems: positive role of the losses *Opt. Express* **21** 21651–68
[14] Hang C, Huang G and Konotop V V 2013 PT symmetry with a system of three-level atoms *Phys. Rev. Lett.* **110** 083604
[15] Sheng J, Miri M, Christodoulides D N and Xiao M 2013 PT -symmetric optical potentials in a coherent atomic medium *Phys. Rev.* A **88** 041803(R)
[16] Morsch O and Oberthaler M 2006 Dynamics of Bose-Einstein condensates in optical lattices *Rev. Mod. Phys.* **78** 179
[17] Schindler J, Li A, Zheng M C, Ellis F M and Kottos T 2011 Experimental study of active LCR circuits with PT-symmetries *Phys. Rev.* A **84** 040101(R)
[18] Lin Z, Ramezani H, Eichelkraut T, Kottos T, Cao H and Christodoulides D N 2011 Unidirectional invisibility induced by PT-symmetric periodic structures *Phys. Rev. Lett.* **106** 213901
[19] Kottos T 2010 Broken symmetry makes light work *Nat. Phys.* **6** 166–7
[20] Ramezani H, Kottos T, El-Ganainy R and Christodoulides D N 2010 Unidirectional nonlinear PT-symmetric optical structures *Phys. Rev.* A **82** 043803
[21] Rüter C E, Makris K G, El-Ganainy R, Christodoulides D N, Segev M and Kip D 2010 Observation of parity-time symmetry in optics *Nat. Phys.* **6** 192–5

[22] Guo A, Salamo G J, Duchesne D, Morandotti R, Volatier-Ravat M, Aimez V, Siviloglou G A and Christodoulides D N 2009 Observation of PT-symmetry breaking in complex optical potentials *Phys. Rev. Lett.* **103** 093902

[23] Kevrekidis P G, Chen Z, Malomed B A, Frantzeskakis D J and Weinstein M I 2005 Spontaneous symmetry breaking in photonic lattices: theory and experiment *Phys. Lett.* A **340** 275–80

[24] Klaiman S, Günther U and Moiseyev N 2008 Visualization of branch points in PT-symmetric waveguides *Phys. Rev. Lett.* **101** 080402

[25] Kartashov Y V, Molamed B A and Torner L 2014 Unbreakable PT symmetry of solitons supported by inhomogeneous defocusing nonlinearity *Opt. Lett.* **39** 19

[26] Lutsky V, Luz E, Granot E and Molamed B A 2018 Making the PT symmetry unbreakable *Parity-time Symmetry and Its Applications* (*Springer Tracts in Modern Physics* vol 280) ed D Christodoulides and J Yang (Singapore: Springer) pp 443–64

[27] Guo D, Xia J, Gu L, Jin H and Dong L 2017 One- and two-dimensional bright solitons in inhomogeneous defocusing nonlinearities with an antisymmetric periodic gain and loss *Physica* D **343** 1–6

[28] Vanin E V, Korytin A I, Sergeev A M, Anderson D, Lisak M and Vázquez L 1994 Dissipative optical solitons *Phys. Rev.* A **49** 2806–11

[29] Tsoy E N, Ankiewicz A and Akhmediev N 2006 Dynamical models for dissipative localized waves of the complex Ginz-burg-Landau equation *Phys. Rev.* E **73** 036621

[30] Yang J 2014 Necessity of PT symmetry for soliton families in one-dimensional complex potentials *Phys. Lett.* A **378** 367–73

[31] Abdullaev F K, Kartashov Y V, Konotop V V and Zezyulin D A 2011 Solitons in PT-symmetric nonlinear lattices *Phys. Rev.* A **83** 041805(R)

[32] Chen Z, Liu J, Fu S, Li Y and Malomed B A 2014 Discrete solitons and vortices on two-dimensional lattices of PT-symmetric couplers *Opt. Express* **22** 29679

[33] Regensburger A, Bersch C, Miri M A, Onishchukov G, Christodoulides D N and Peschel U 2012 Parity-time synthetic photonic lattices *Nature* **488** 167–71

[34] Makris K G, Ge L and Türeci H E 2014 Anomalous transient amplification of waves in non-normal photonic media *Phys. Rev.* X **4** 041044

[35] Syms R and Cozens J 1992 *Optical Guided Waves and Devices* (London: McGraw-Hill)

[36] Barashenkov I V and Gianfreda M 2014 An exactly solvable PT-symmetric dimer from a Hamiltonian system of nonlinear oscillators with gain and loss *J. Phys. A: Math. Theor.* **47** 282001

[37] Chen Y, Snyder A W and Payne D N 1992 Twin core nonlinear couplers with gain and loss *IEEE J. Quantum Electron.* **28** 239–45

[38] Miri M A, LiKamWa P and Christodoulides D N 2012 Large area single-mode parity-time-symmetric laser amplifiers *Opt. Lett.* **37** 764–6

[39] Li R, Li L and Li P 2013 Asymmetric optical amplifier based on parity-time symmetry *Proc. Rom. Acad. Math. Phys. Tech. Sci. Inf. Sci.* **14** 121–6 (https://acad.ro/sectii2002/proceedings/doc2013-2/06-LI.pdf)

[40] Yang X and Wong C W 2007 Coupled-mode theory for stimulated Raman scattering in high-Q/V_m silicon photonic band gap defect cavity lasers *Opt. Express* **15** 4763–80

[41] Agarwal G P 2001 *Nonlinear Fiber Optics* 3rd edn (Florida: Academic)

[42] Karthiga S, Chandrasekar V K, Senthilvelan M and Lakshmanan M 2017 Controlling of blow up responses by nonlinear PT-symmetric coupling *Phys. Rev.* A **95** 033829

[43] Menotti M, Morrison B, Tan K, Vernon Z, Sipe J E and Liscidini M 2019 Nonlinear coupling of linearly uncoupled resonators *Phys. Rev. Lett.* **122** 013904

[44] Hassan A U, Hodaei H, Miri M A, Khajavikhan M and Christodoulides D N 2016 Integrable nonlinear parity-time-symmetric optical oscillator *Phys. Rev.* E **93** 042219

[45] Barashenkov I V, Jackson G S and Flach S 2013 Blow-up regimes in the PT-symmetric coupler and the actively coupled dimer *Phys. Rev.* A **88** 053817

[46] Pickton J and Susanto H 2013 Integrability of PT-symmetric dimers *Phys. Rev.* A **88** 063840